

Exciton dissociation in polymer field-effect transistors studied using terahertz spectroscopy

J. Lloyd-Hughes,^{1,*} T. Richards,² H. Sirringhaus,² M. B. Johnston,¹ and L. M. Herz^{1,†}

¹Claredon Laboratory, Department of Physics, University of Oxford, Parks Road, Oxford OX1 3PU, United Kingdom

²Cavendish Laboratory, Department of Physics, University of Cambridge, Madingley Road, Cambridge CB3 0HE, United Kingdom

(Received 9 October 2007; revised manuscript received 26 January 2008; published 7 March 2008)

We have used terahertz time-domain spectroscopy to investigate photoinduced charge generation in conjugated polymer field-effect transistors. Our measurements show that excitons dissociate in the accumulation layer under the application of a gate voltage, with a quantum efficiency of ~ 0.1 for an average gate field of $\sim 1 \times 10^8 \text{ V m}^{-1}$. The transistor history is found to affect the exciton dissociation efficiency, which decreases as holes are increasingly trapped in the accumulation layer. The quantum efficiency of charge formation from excitons is compared with the two contrasting models proposed by Onsager and Arkhipov based on the assumption that field-induced exciton dissociation is assisted by the Brownian diffusive motion or an initial excess energy supplied by excited vibrational modes, respectively.

DOI: [10.1103/PhysRevB.77.125203](https://doi.org/10.1103/PhysRevB.77.125203)

PACS number(s): 72.80.Le, 71.35.Aa, 78.47.-p

I. INTRODUCTION

Conjugated polymers are increasingly finding applications in flexible solar cells,^{1,2} transistors,^{3,4} and light-emitting diodes (LEDs)⁵ because of their versatile optoelectronic and mechanical properties. One outstanding challenge to the efficient operation of organic solar cells and phototransistors is the often low quantum yield of charge formation from photoexcited excitons. A number of mechanisms for exciton dissociation in conjugated polymers have been evoked, which have conventionally been separated into the so-called *intrinsic* and *extrinsic* effects.⁶ Here, *intrinsic* generation of charge carriers refers to the direct creation of free charges in the bulk of the polymer. *Extrinsic* charge generation may result from the dissociation of excitons at defects, interfaces, or charge-injection contacts. Efficient solar cells rely largely on extrinsic charge generation at a heterojunction between two materials whose energy levels are optimized for fast transfer of one charge across the interface.^{1,2,7} For this case, the efficiency of exciton dissociation into charges is typically high and is critically influenced by the blend morphology.⁸

In contrast, exciton dissociation efficiencies in neat polymer films tend to be low, most likely as a result of the high exciton binding energy for organic semiconductors.⁹ A number of mechanisms for charge generation in bulk polymer films have been proposed and are still an ongoing matter of debate. The observation of an onset of charge separation for excitation energies near the low-energy edge of the absorption spectrum has alternately been attributed to charge generation at defects, impurities and the electrodes,¹⁰ to the presence of energetic disorder,¹¹ and a lamellar chain arrangement.¹² A rapid increase in charge generation efficiency observed at energies of $\sim 1 \text{ eV}$ above the absorption edge has been interpreted both in terms of “hot” exciton dissociation aided by excess vibrational energy^{13,14} and a change in the quantum mechanical nature of the excitonic state accessed in the transition.^{15,16} In addition, the presence of an electric field lowers the Coulombic barrier for charge separation, which has been shown to cause a substantial increase in the exciton dissociation efficiency.^{17,18} Finally, at very high photon fluences ($>100 \mu\text{J cm}^{-2}$ within a 100 fs

pump pulse), two-step processes may directly generate a significant fraction of free charges via excitonic intermediary states.^{16,19}

Examinations of electric-field-induced exciton dissociation in conjugated polymer films have typically been conducted using devices based on LED structures. However, such measurements are often hampered by extrinsic charge generation at the contacts, which can significantly influence the measured photocurrents.^{6,10,20} For polymer field-effect transistors (pFETs) fabricated on an insulated gate, such effects are less likely to play a role, as typical channel lengths are substantially larger, and the gate contact is electrically well insulated from the polymer. Illumination of pFETs has been reported to increase their source-drain current^{21,22} and also to remove trapped holes.^{23,24} For a better understanding of the mechanism underlying the photocurrent generation, a study into exciton dissociation in pFETs is urgently required. While current-voltage characteristics are undoubtedly the measure of device performance, their usefulness in determining charge carrier densities and mobilities is often hampered by contact resistance effects.^{25,26} Parasitic capacitances can also make the quantitative determination of charge densities from capacitance measurements a challenge.

Here, we examine the mechanism by which excitons dissociate in thin films of a conjugated polymer incorporated into a pFET device structure. We use a noncontact spectroscopic technique based on terahertz (far infrared) radiation ($1 \text{ THz} \equiv 300 \mu\text{m} \equiv 33.3 \text{ cm}^{-1}$) to measure the charge density of holes in the polymer at room temperature. We find that a significant hole population is generated under illumination in the presence of an applied gate voltage, with no source-drain bias. The charge generation efficiency is determined, and it is compared with two contrasting models, taking into account the electric-field distribution in the polymer.

II. EXPERIMENTAL TECHNIQUE

Terahertz time-domain spectroscopy (TDS) can be used to determine the conductivity of quasiparticles in materials as diverse as high temperature superconductors²⁷ and semiconductor nanowires.²⁸ In a previous study,²⁶ we reported that

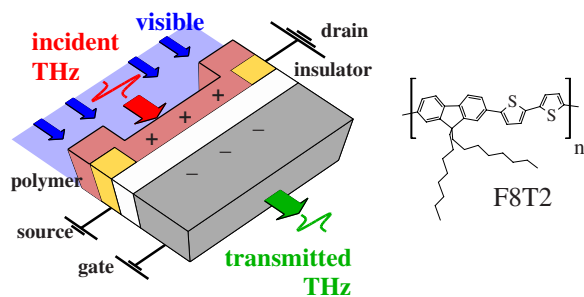


FIG. 1. (Color online) Experimental setup used to perform terahertz time-domain spectroscopy on polymer transistors, described in Sec. II. One unit of the source and/or drain interdigitated array is shown. The hole and electron accumulation layers in the polymer and gate are represented by + and -. The polymer was illuminated with light in the visible frequency range from various LEDs. The monomer unit of the polymer F8T2 is also shown.

terahertz TDS can track the charge density of trapped holes in the accumulation layer of poly[(9,9-dioctylfluorene-2,7-diyl)-co-(bithiophene)] (F8T2) polymer transistors with a silicon gate. The experimental scheme was to measure the change in the terahertz pulse transmitted through the transistor induced by a gate-voltage modulation V_g at 40 Hz, as shown schematically in Fig. 1. The absolute change in transmission $|\Delta T/T|$ is defined as $|\Delta T/T| = |(T_{V_g} - T_0)/T_0|$, where T_{V_g} and T_0 are, respectively, the transmission with and without a gate voltage. The frequency dependence of $|\Delta T/T|$ was found to be consistent with absorption by free carriers in the “mirror accumulation layer” in the silicon gate. Probing the conductivity and associated density of this electron layer in silicon thus allowed the corresponding hole density in the polymer to be monitored during device degradation. A significant and nonreversible hole trapping was seen to cause a substantial buildup of charge density in the polymer during the “off” state, reducing $|\Delta T/T|$ exponentially with a lifetime of 7×10^3 s. It was found that $|\Delta T/T| \propto n_{\text{on}} - n_{\text{off}}$, where n_{on} and n_{off} are the hole density with and without an applied gate voltage, respectively. As a consequence of charge trapping, the transistor’s threshold voltage for source-drain current flow increases during the degradation process.⁴

For the work reported here, we have used an extension of this terahertz TDS technique to investigate the creation of additional holes in the polymer transistor as a result of photoexcitation. The experimental setup was described in Ref. 26, but with the following modifications. First, prior to measurements, a gate-voltage modulation $V_g = 0 \leftrightarrow -30$ V was applied at 40 Hz for 10^5 s, after which time the available hole traps in the polymer film were fully populated.²⁶ This was performed in order to reach an equilibrium state and thus prevent a change in the trapped charge density from influencing the photoexcitation experiments.²⁹ The polymer thin film was then illuminated with light from a variety of high-power LEDs with peak wavelengths ranging from $\lambda = 636$ to 396 nm (or photon energies $E_\gamma = 1.95$ – 3.13 eV) for a period of 100 s. The change in transmission $|\Delta T/T|$ was recorded (using a lock-in amplifier) and averaged over 5 s intervals before, during, and after the application of the light.

The experimental method and the associated data analysis may be considered to be a cw version of recently presented ultrafast optical-pump terahertz-probe measurements.^{28,30,31} All measurements were performed at room temperature, with the transistors and terahertz system under a vacuum of $< 10^{-3}$ mbar. The spectral emission characteristic of each LED was measured using an Ocean Optics fiber-optic spectrometer.

The series of polymer transistors used were fabricated as follows. A layer of F8T2 was deposited through spin casting from solution onto an interdigitated gold array (which had a 40 μm channel length, 50 μm finger width, and total channel width of 45 mm). A 200-nm-thick layer of SiO_2 electrically insulated the polymer from the gate electrode, which comprised of a lightly *n*-doped silicon wafer ($2.5 \times 10^{15} \text{ cm}^{-3}$) with a total thickness of 0.62 mm. The thickness of each polymer film was measured using a surface profilometer. Transfer and output current-voltage characteristics were measured to monitor the transistor action of the devices under negative gate voltage bias. Additionally, the source-drain current was measured before, during, and after illumination in an analogous experiment to the spectroscopic study using terahertz spectroscopy.

III. EXPERIMENTAL RESULTS

A. Influence of excitation energy

Figure 2(a) shows the gate-voltage induced change in terahertz transmission $|\Delta T/T|$ as a function of time t . $|\Delta T/T|$ was typically about 10^{-3} . At $t=0$ illumination of the transistor with an LED is started and is stopped 100 s later. For illumination at $\lambda = 396$ nm (purple squares), an $\sim 40\%$ step increase in $|\Delta T/T|$ can be seen within 1 s of LED turn on, while illumination at $\lambda = 636$ nm (red crosses) induces no change. For the latter case, the transmission energy is below the absorption edge of F8T2 but above the indirect band gap energy of silicon, suggesting that photoexcitation of the silicon gate can be ruled out as a mechanism for the transmission changes. To examine the excitation-energy dependence of the light-induced enhancement of $|\Delta T/T|$ in more detail, measurements were conducted using a range of LEDs, with spectra shown in Fig. 3. Defining $\Delta = |\Delta T/T|_{\text{LED on}} - |\Delta T/T|_{\text{LED off}}$, Δ is found to scale linearly with the incident photon fluence (not shown). The open circles in Fig. 3 show Δ after normalization by the incident photon flux. It can be seen that Δ tracks the S_0 to S_1 excitonic absorption spectrum of F8T2 (solid line). The light-induced enhancement in $|\Delta T/T|$ must therefore be a consequence of the photogeneration of excitons in the polymer film.

A direct influence of the photoexcited exciton population on $|\Delta T/T|$ can be ruled out for the following reasons. While the generation of excitons in conjugated polymer films has been shown to alter its transmissivity in the terahertz frequency range,³² this change is expected to be insignificant in comparison to that caused by free carriers in silicon. An estimate of the excitonic contribution to $|\Delta T/T|$ of less than 10^{-8} may be obtained by scaling the values obtained previously for such excitonic contributions,³² taking into account the equilibrated exciton densities used in the present study. In

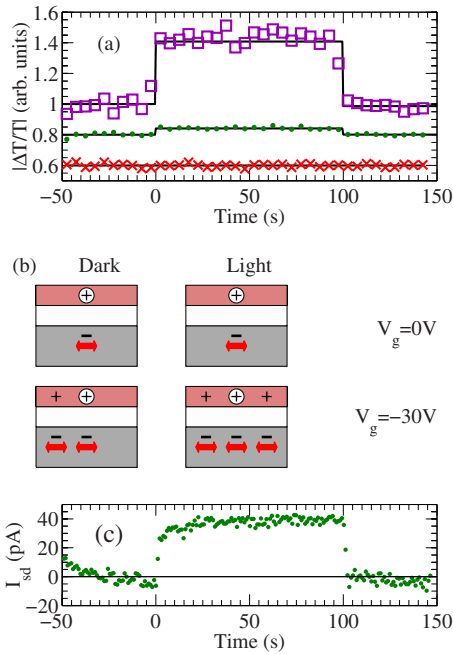


FIG. 2. (Color online) (a) Change in transmitted terahertz radiation pulse $|\Delta T/T|$ induced by a gate-voltage modulation $V_g=0 \leftrightarrow -30$ V at 40 Hz. At zero time, a near-UV LED ($\lambda=396$ nm) illuminates the polymer, increasing $|\Delta T/T|$ (squares, normalized to its preillumination value) until LED turn off 100 s later. The same experiment was repeated at comparable irradiances using a variety of LEDs, including a green LED (points, $\lambda=542$ nm, offset vertically by -0.2 for clarity) and a red LED (crosses, $\lambda=636$ nm, offset by -0.4). The solid lines are guides for the eyes. (b) Schematic of mobile (+) and trapped (\oplus) holes in polymer and electrons (-) in the gate without (top) and with (bottom) an applied gate voltage in the dark (left) and light (right). (c) Source-drain current at $V_g=-30$ V, $V_{sd}=5$ V, under illumination with the $\lambda=542$ nm LED from 0 to 100 s. The nonzero source-drain current between -50 and -40 s is a result of the removal of trapped holes in the dark (Ref. 24), which occurred during the period when the source measurement unit was connected, when no gate voltage was applied to the transistor.

comparison, the observed values of $|\Delta T/T|$ are around 10^{-3} , which is larger by several orders of magnitude. In addition, the use of a lock-in technique means that only a difference in the photogenerated carrier density induced by the applied gate-voltage modulation is detected.

The observed enhancement in $|\Delta T/T|$ during photoexcitation can therefore be attributed to an altered hole charge density in the channel, either an increase in n_{on} or a reduction in n_{off} , since $|\Delta T/T| \propto n_{on} - n_{off}$ for the presented measurements.²⁶ A reduction in n_{on} could, in principle, be caused by a photoinduced removal of trapped carriers. However, as we have recently demonstrated for this type of transistor,²⁶ after illumination is turned off, refilling of traps would then be expected to occur over a time scale of ~ 7000 s, significantly longer than the time scales observed in Fig. 2. The measurements presented in Fig. 2(a) show instead that $|\Delta T/T|$ returns to its preillumination value within 1 s, suggesting that hole detrapping does not make a signifi-

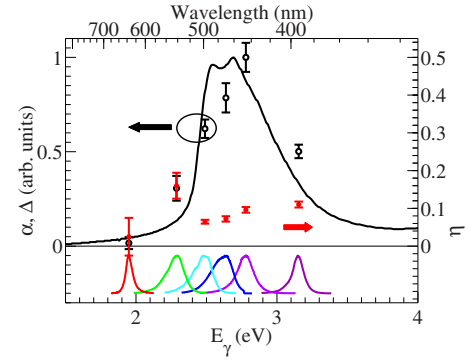


FIG. 3. (Color online) Light-induced change in $|\Delta T/T|$ at a gate-voltage modulation $V_g=0 \leftrightarrow -30$ V (hollow points, left-hand y axis), defined as $\Delta = |\Delta T/T|_{LED\ on} - |\Delta T/T|_{LED\ off}$, divided by the incident photon flux at various illumination wavelengths. Δ has been normalized with respect to its value at 2.78 eV excitation energy. Also shown are the absorption α of F8T2 (solid line, from thin-film transmission measurements) and the quantum efficiency η (points, right-hand y axis, obtained as described in the text). The measured LED emission spectra are plotted at the bottom.

cant contribution to the observed effects. Several previous studies have reported that photoexcitation can aid the recovery of polymer transistors whose threshold voltage had increased the following charge trapping.^{23,24} However, we observe no permanent detrapping at these excitation fluences and on these time scales. We therefore propose that the observed changes are rather the result of an increase in n_{on} following photoexcitation. This interpretation is in analogy to previous studies of F8T2^{22,33} and pentacene³⁴ transistors, which have indicated that illumination above the absorption edge generates an enhanced source-drain current over the dark state, even with no applied gate voltage (no channel), a finding attributed to the dissociation of excitons. For the measurement technique presented here, an increase in n_{on} under illumination can create a larger $|\Delta T/T|$ only if the exciton dissociation efficiency is larger with an applied V_g than without. As a result, the contribution to the light-induced changes in $|\Delta T/T|$ from exciton dissociation at interfaces and defects should be minimal.

The proposed mechanism for the observed change in $|\Delta T/T|$ under illumination is illustrated schematically in Fig. 2(b). The left-hand side of the graphic illustrates the case prior to illumination. For $V_g=0$ V (top), only trapped holes (labeled \oplus) are present in the polymer layer, matched by an equal density of mobile electrons (-) in the silicon. The lower-left plot shows that upon application of $V_g=-30$ V, mobile holes (+) are created in the accumulation layer of the polymer transistor. The electron density in the silicon increases correspondingly and reflects the total density of both trapped and mobile holes in the polymer. This change in electron density is the cause of the change in the transmission of terahertz radiation upon applied gate voltage.²⁶ Following illumination [right-hand side of Fig. 2(b)], a fraction of photogenerated excitons may dissociate into free carriers under the application of an electric field. After exciton dissociation has occurred, the electron will drift through the

bulk away from the channel and may be swept out of the transistor or eventually recombine with a hole. The hole originating from the dissociated exciton will be attracted toward the transistor's channel when a field is applied. Exciton dissociation will therefore lead to an enlarged hole density during an applied gate voltage V_g with a matching increase in the electron density in the silicon gate, thus enhancing $|\Delta T/T|$.

The enhanced hole density after dissociation of photoexcited excitons allows a current to flow on the application of a source-drain voltage V_{sd} . At a constant $V_g = -30$ V and $V_{sd} = -5$ V, the measured source-drain current (for a transistor with saturated hole traps, as above) is plotted in Fig. 2(c). Before illumination, I_{sd} is negligible because the threshold voltage exceeds V_g , as evidenced by the transfer characteristics of our transistors (not shown, similar to those in Ref. 23). In agreement with the terahertz spectroscopy results, the current is enhanced under illumination at 542 nm during the period of 0–100 s. Previous photocurrent studies have demonstrated that the photocurrent tracks the absorption spectrum of F8T2.²² The photocurrent in Fig. 2(c) rapidly returns to zero at $t = 100$ s, indicating that no substantial detrapping of holes occurred under illumination.

In a previous study of pFETs using terahertz spectroscopy, we were able to demonstrate that the electron density in the silicon gate may be extracted from the measured $|\Delta T/T|$ using a simple Drude–Lorentz model.²⁶ We use the same approach here in order to determine the photoinduced change in electron density in the silicon and the corresponding photo-generated increase in the hole density n_{ind} within the polymer transistor channel. Typical values extracted in this manner for excitation with a fluence of 7×10^{-3} W cm⁻² near the peak of the absorption and for an applied gate voltage of -30 V are around $n_{ind} \sim 2 \times 10^{11}$ cm⁻².

In order to obtain the external quantum efficiency for exciton dissociation η from the photoinduced hole density at each excitation wavelength, we used the following approach. For holes decaying with lifetime τ , the change in n_{ind} can be described by the rate equation $dn_{ind}/dt = \eta G - n_{ind}/\tau$. Here, G is the absorbed photon flux calculated from

$$G = T\{\exp[-\alpha(d - \delta)] - \exp[-\alpha d]\}n_\gamma, \quad (1)$$

where n_γ is the incident photon flux, α the absorption coefficient, $d = 30$ nm the polymer film thickness, and $T = 0.61$ accounts for the Fresnel reflection losses. This form of the absorbed photon flux is required if exciton dissociation occurs with a distance $\delta = 5$ nm of the polymer and/or insulator boundary, which is indeed shown to be the case in Sec. III C. The solution to the above rate equation for the hole density is $n_{ind}(t) = \eta G \tau (1 - \exp[-t/\tau])$. The recombination of photoexcited holes in F8T2 has been measured using transient absorption spectroscopy,² where nonexponential decays were seen with a substantial hole population 1 ms after photoexcitation, but not after 1 s. Here, we approximate the decay as exponential with a lifetime $\tau = 1$ ms, resulting in

$$n_{ind} = \eta G \tau \quad (2)$$

in the limit that the period with V_g on (12.5 ms) is significantly larger than τ (1 ms). This value of τ is consistent with

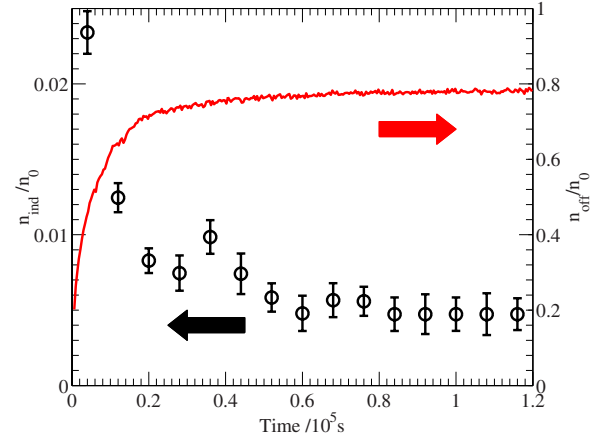


FIG. 4. (Color online) The photoinduced carrier density n_{ind} (points, left-hand axis, $E_\gamma = 2.29$ eV) during hole trapping for a pristine transistor normalized by the hole density in the absence of light, $n_0 = 3.2 \times 10^{12}$ cm⁻² ($V_g = 0 \leftrightarrow -30$ V). The trapped hole density n_{off} (solid line, right-hand axis) is also shown. The data shown in all other figures were obtained at times after 1.2×10^5 s, when the photoinduced carrier density is constant.

the observed rapid equilibration of $|\Delta T/T|$ after illumination begins and with the rapid return of $|\Delta T/T|$ to its preillumination value on the removal of the illumination [Fig. 2(a)]. If the lifetime was of the order of 12.5 ms (or larger), then the photoinduced carriers would remain during the period with V_g off, and the terahertz modulation signal $|\Delta T/T|$ would be negligible. The values for the quantum efficiency η extracted from the changes in the terahertz transmission using Eq. (2) are shown in Fig. 3 (points) as a function of excitation energy. Across the lowest π - π^* absorption band ($2.5 < E_\gamma < 3.5$ eV), η is roughly constant and of the order of 0.1 at the set gate voltage $V_g = -30$ V. Such excitation-energy insensitive behavior of η has previously also been observed in photocurrent studies of a ladder-type polyparaphenylene⁶ and for microwave conductivity measurements of polythiophene,¹² for which it has been attributed to extrinsic and intrinsic charge-dissociation mechanisms, respectively.

B. Effects of transistor history

To examine the effects of transistor history on exciton dissociation in F8T2, the photoinduced carrier density n_{ind} was measured as a function of operating time for a pristine transistor. Light periods of 100 s were followed by dark periods of 100 s, as in Fig. 2. In Fig. 4, the solid line indicates the trapped hole density n_{off} (measured during the dark periods), which initially increases exponentially before saturating at the available trap density.²⁶ Also shown is the value of n_{ind} measured during this period for $E_\gamma = 2.29$ eV. As more and more holes become trapped, the magnitude of n_{ind} decreases to about one-quarter of the value for the pristine transistor before equilibrating after 10^5 s. This behavior is similar to that observed for anthracene single crystals for which carrier trapping was found to reduce η at low applied fields.²⁹ The mechanism for this moderate reduction in n_{ind} with trapped hole density is not clear, but if excitonic disso-

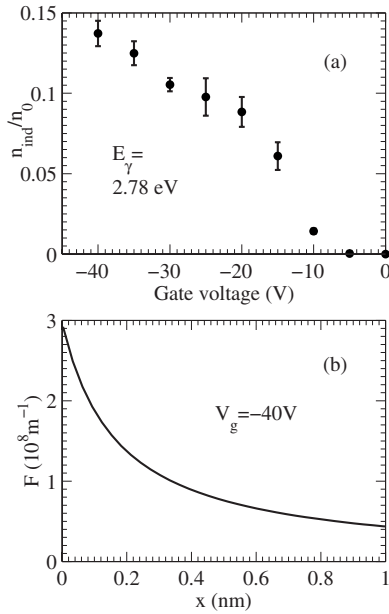


FIG. 5. (a) Gate-voltage dependence of the photoinduced carrier density n_{ind} (points), obtained as described in the text. The initial value of the mobile charge density at $V_g = -30$ V was $n_0 = 3.2 \times 10^{12} \text{ cm}^{-2}$. (b) Calculated electric-field distribution $F(x)$ (solid line, left y axis) versus depth x from the polymer-insulator boundary at $V_g = -40$ V.

ciation at impurity sites was significant, then n_{ind} ought to remain constant with measurement time (for a constant impurity density) or even increase (for dissociation at defects generated by hole trapping), neither of which are observed. Possibly, a shorter hole polaron lifetime at greater trapped hole densities is responsible for the decrease in n_{ind} [Eq. (2)]. Alternatively, n_{ind} may be larger at early times owing to negligible screening of the applied electric field when the trapped hole density is small. As these pFETs are prone to showing such degradation effects very soon after turn on, the data presented in all other sections of this paper were taken once the transistor had equilibrated and all trap sites were filled.

C. Effect of gate voltage

The photoinduced generation of additional holes in the transistor measured at the frequency of the gate modulation strongly suggests that excitons are dissociated through assistance by the gate electric field. Several previous studies have shown that under a large electric field ($> 10^7 \text{ V m}^{-1}$), excitons can be spontaneously separated, forming a geminate electron-hole pair.¹⁷ In order to investigate the mechanism of exciton dissociation, we measured the photoinduced change in the hole density n_{ind} as a function of the gate-voltage modulation depth V_g , as shown in Fig. 5(a). For an excitation energy $E_\gamma = 2.78 \text{ eV}$, the measured n_{ind} (points) increases with increasingly negative gate voltage and reaches significant values only once a voltage $V_g = -10$ V is passed.

An assessment of the effect of an electric field on the exciton dissociation efficiency requires the electric-field dis-

tribution inside the polymer film to be known. For this purpose, the electric-field strength F at a given experimental gate voltage was obtained by solving Poisson's equation at a distance x from the polymer-insulator boundary (see, e.g., Ref. 35 for a derivation). An example of the obtained field distribution is shown in Fig. 5(b) for $V_g = -40$ V. The gate insulator lies at $x < 0$, and the solution was performed over the polymer film's full thickness (30 nm) although only the high field region is shown here. $F(x)$ can be seen to decrease from $3 \times 10^8 \text{ V m}^{-1}$ at the polymer and/or insulator interface to $4 \times 10^7 \text{ V m}^{-1}$ at 1 nm. In order to obtain a reference value against which the exciton dissociation efficiencies could be plotted, the mean field strength $\langle F \rangle$ was calculated over the range of $0 \leq x \leq 1$ nm (the approximate width of the accumulation layer) for each value of the experimentally applied V_g . For instance, at $V_g = -40$ V, $\langle F \rangle = 9.7 \times 10^7 \text{ V m}^{-1}$, while the average field from $1 \leq x \leq 30$ nm is only $5.7 \times 10^6 \text{ V m}^{-1}$. The increase in exciton dissociation for $V_g < -10$ V and the modeling described in the next section suggest that most of the exciton dissociation occurs in the high-field region of the accumulation layer, making $\langle F \rangle$ a suitable choice. However, diffusion of excitons during their lifetime occurs over nanometer scale distances in conjugated polymer films and will affect the effective thickness of the layer for which absorbed excitons are able to experience the high-field region and dissociate with high probability. We have taken into account these effects through Eq. (1) by assuming as an approximation that excitons generated within the diffusion length δ (taken as $\delta \sim 5$ nm for F8T2³⁶) away from the gate contact are able to experience the calculated average field $\langle F \rangle$.

The quantum yield η was extracted from the experimental data for n_{ind} using Eq. (2) in the same manner, as described in Sec. III A. The resulting values of η are displayed as a function of the average field in the accumulation layer $\langle F \rangle$ in Figs. 6(a) and 6(b) for excitation energies $E_\gamma = 2.78 \text{ eV}$ and $E_\gamma = 2.29 \text{ eV}$, respectively. The observed quantum yields are of the order of $\eta \sim 0.1$, which is consistent with typical values found for field-induced exciton dissociation in diode device structures. Previous measurements of this kind have determined a value of $\eta = 3 \times 10^{-1}$ for a polyphenylenevinylene-amine¹⁴ at $F = 1 \times 10^8 \text{ V m}^{-1}$, while $\eta = 10^{-3}$ for a ladder-type polyphenylene.¹³

IV. MODELING AND DISCUSSION

In the previous section, it was established that the photoinduced charge density in F8T2 polymer transistors depends on the applied gate voltage. A number of approaches to modeling the yield of field-induced dissociation η at a given electric-field strength F have been used in recent years. In order to compare our experimentally determined charge-dissociation efficiencies with theory, we focus here on the two substantially different models of Onsager³⁷ and Arkhipov *et al.*^{13,14} The two approaches are described in Secs. IV A and IV B before their application to our experimental data is discussed in Sec. IV C.

A. Onsager model

In the Onsager model, the quantum yield is calculated assuming that excitons autoionize into an intermediate state

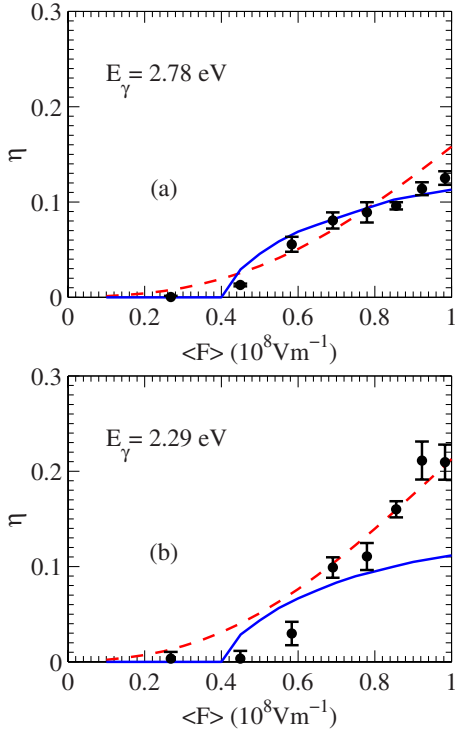


FIG. 6. (Color online) Experimental quantum yield η against average field $\langle F \rangle$ for photon excitation energies of (a) 2.78 eV and (b) 2.29 eV (points). Also shown are $\eta(\langle F \rangle)$ calculated using the Onsager model (dashed lines) and the Arkhipov model (solid lines).

with electron-hole separation r_0 , known as the thermalization distance or the Onsager radius.^{37,38} The probability for this to occur is η_0 , and it is assumed to be independent of electric field. Charges then undergo Brownian motion within a Coulombic potential well modified by the applied field F . Onsager established that under these assumptions, the dissociation efficiency from the intermediate state is proportional to a Boltzmann factor containing the ratio of the charges' kinetic energy to the Coulomb binding energy.³⁷ The quantum efficiency η for free charge formation from excitons may then be written as³⁸

$$\eta(r_0, F) = \eta_0 \frac{kT}{eFr_0} e^{-A} e^{-eFr_0/kT} \sum_{m=0}^{\infty} \frac{A^m}{m!} \sum_{n=0}^{\infty} \sum_{l=m+n+1}^{\infty} \left(\frac{eFr_0}{kT} \right)^l \frac{1}{l!}, \quad (3)$$

where $A = e^2/4\pi\epsilon\epsilon_0 kTr_0$ for a material with relative dielectric constant ϵ at a temperature T . This form of the Onsager model is valid for an isotropic medium such as F8T2, a nematic liquid crystal. The model has previously been used to reproduce successfully the field dependence of η measured for thin films of polyphenylenevinylene.^{10,20} To provide fits to the experimental data, Eq. (3) was evaluated numerically to high convergence, with the sums terminated at $m=n=20$ and $l=50$.

B. Arkhipov model

Alternatively, the approach of Arkhipov *et al.*¹³ assumes that exciton dissociation occurs on ultrafast (~ 100 fs) time

scales. Here, the initial exciton distribution has a temperature above ambient and subsequently dissipates this excess energy into vibrational modes. Only during the initial time period when the average excitonic vibrational energy $\langle E \rangle$ exceeds the Coulombic energy barrier carriers can excitons separate. It is further assumed that once the exciton is separated, carriers cannot recombine and may contribute to the photoconductivity. For an initial excess exciton energy $\langle E_0 \rangle$ the exciton dissociation efficiency is then calculated as¹³

$$\eta(\langle E_0 \rangle, F) = \int_{z_{\min}}^1 dz \left\{ 1 - \exp \left[- \frac{\nu_0}{\beta} \int_0^{\langle E_0 \rangle} d\langle E \rangle \right] \times \text{Bol} \left(\frac{E_b}{\langle E \rangle} - \frac{e}{\langle E \rangle} \sqrt{\frac{eFz}{\pi\epsilon\epsilon_0}} \right) \right\}, \quad (4)$$

where $\text{Bol}(x < 0) = 1$ and $\text{Bol}(x > 0) = \exp(-x)$, E_b is the exciton binding energy, and ν_0/β is the ratio of the electron-phonon coupling strength ν_0 to the rate β at which the excess energy is (linearly) dissipated with time. The integration is over $z = \cos \phi$, where ϕ is the angle between the polymer segment of length L and the applied electric field. The lower limit of the integral is $z_{\min} = e/4\pi\epsilon\epsilon_0 L^2 F$, and it is set by assuming that no exciton dissociation can occur unless the electric-field component along the chain ($F \cos \phi$) is greater than the Coulomb field required to separate charges by the distance L . The model has previously been shown to reproduce the experimentally determined field dependence of η for thin films of a ladder-type polyparaphenylene and a polyphenylenevinyleneamine.¹⁴ In order to evaluate Eq. (4) accurately to fit our data, each integral was performed as a summation with 100 steps.

C. Comparison of theory with experiment

To compare the two theoretical models to the experimental data, the following approach was taken. The theoretical curves from the models were evaluated over a range of electric-field strengths, up to the maximum of the average electric field $\langle F \rangle$ at $V_g = -40$ V. The obtained curves for $\eta(\langle F \rangle)$ are shown in Fig. 6 for the models of Arkhipov (solid lines) and Onsager (dashed lines) together with the data for illumination at 2.29 and 2.78 eV. For both models, significant quantum efficiency is obtained only above a field strength of 4×10^7 V m⁻¹. This justifies the assumption made in Sec. III C that only the accumulation layer contributes to exciton dissociation.

The parameters used for the theoretical curves in Figs. 6(a) and 6(b) are summarized in Table I. Considering first the results obtained for the Onsager model, Fig. 6 shows that theoretical values obtained for η increase rapidly with F in reasonable agreement with the experimental data for $E_\gamma = 2.78$ eV and for $E_\gamma = 2.29$ eV. The thermalization distance obtained from the fits ($r_0 = 2.10$ nm for $E_\gamma = 2.78$ eV and $r_0 = 2.25$ nm for $E_\gamma = 2.29$ eV) is comparable to the length of the monomer unit for F8T2 (1.6 nm). This value seems realistic as quantum chemical calculations suggest that the extent of the relaxed S_1 excitonic wave function in typical conjugated polymers is of the order of one monomer unit.¹⁵ The

TABLE I. Parameters used in the Onsager–Arkhipov models of quantum efficiency, as defined in Secs. IV A and IV B. The calculated quantum efficiencies are shown in Fig. 6.

	Onsager		Arkhipov	
E_γ	2.29 eV	2.78 eV		2.78 eV
r_0	2.25 nm	2.10 nm	l	3.4 nm
ϵ	3	3	ϵ	3
T	296 K	296 K	$\langle E_0 \rangle$	0.25 eV
η_0	1.0	1.0	ν_0/β	0.9 eV ⁻¹
			E_b	0.3 eV

experimental data shown in Fig. 3 demonstrate that the measured quantum yield is roughly constant over the range of excitation energies ($2.29 \text{ eV} < E_\gamma < 3.13 \text{ eV}$). Within Onsager's theory, this finding corresponds to a constant thermalization radius across the lowest excitonic absorption band of the order of $r_0 = 2.0\text{--}2.3 \text{ nm}$.

The theoretical fits based on the Arkhipov model correspond well to the experimental data for $E_\gamma = 2.78 \text{ eV}$, as shown in Fig. 6(a). To reproduce $\eta(\langle F \rangle)$, an exciton binding energy of 0.3 eV was used, the value for polydiocylfluorene obtained from scanning tunneling microscopy.³⁹ The conjugation length of a segment was extracted from the fits as $L = 3.4 \text{ nm}$. This parameter is relatively sensitive to the data as it is determined by the rapid onset in dissociation that occurs when the critical applied field strength $4 \times 10^7 \text{ V m}^{-1}$ is exceeded (see Fig. 6). The assumption of a critical field taken in the Arkhipov model hence enables a better fit to the experimental data at low gate voltages ($|V_g| < 10 \text{ V}$) than the Onsager model. However, the sharp onset of η may partly be the result of trapped charge present in the accumulation channel.²⁹ The ratio of the electron-phonon coupling strength to the dissipation rate was taken from Ref. 13 as $\nu_0/\beta = 0.9 \text{ eV}^{-1}$. The initial thermal excess energy was extracted as $\langle E_0 \rangle = 0.25 \text{ eV}$, which (as in Refs. 13 and 14) is a fit parameter rather than being derived from the excitation energy used in the experiment. The value obtained for $\langle E_0 \rangle$ is larger than typical values extracted when the theory was originally applied to model exciton dissociation in ladder-type polyparaphenylene.¹³ This previous study only found modest increases of $\sim 0.05 \text{ eV}$ in the theoretically extracted excess thermal energy per increase of 1 eV in the excitation energy. However, we find that the value of $\langle E_0 \rangle$ also depends sensitively on the choice of the energy dissipation rate: we were able to obtain an equally good fit to the experimental data in Fig. 6(a) using $\nu_0/\beta = 0.45 \text{ eV}^{-1}$ and $\langle E_0 \rangle = 0.4 \text{ eV}$. Regardless of the exact value of $\langle E_0 \rangle$, the energy independence of the experimental $\eta(\langle F \rangle)$ over the S_1 absorption band (Fig. 3) implies that a hot exciton dissociation model is not really appropriate here.

Overall, a comparison between the two models is challenging, as both rely on a set of assumptions with opposite extremes. The model developed by Arkhipov *et al.* suggests that an exciton only has a chance of dissociation during the lattice relaxation period of the first 100 fs. More importantly,

it suggests that once an exciton has overcome the Coulombic barrier to dissociation, it remains dissociated. This assumption seems at odds with experimental work that has identified charge recombination as a limiting factor to maintaining a high photocurrent even for material blends optimized to maintain a charge separated state.⁴⁰ The Arkhipov model appears to work well for the part of the photocurrent spectrum where charge dissociation increases monotonically with increasing excitation energy.^{13,14} However, other studies conducted over a wider range of excitation energies have found nonmonotonic dissociation efficiency spectra displaying plateaus and peaks that may correlate with particular features in the absorption spectra.^{15,12,16} These studies suggest that an Onsager model in which the thermalization radius is dependent on the quantum mechanical state accessed in the transition may be more appropriate to account for the whole photocurrent spectrum. Quantum chemical calculations have shown that electronic transitions from delocalized occupied molecular orbitals to localized unoccupied levels and vice versa may be particularly likely to result in exciton dissociation.¹⁵ For such excitations, the electron and the hole have a significantly higher probability of spending time apart, corresponding to a larger thermalization radius in the Onsager model.

The discrepancies between the Onsager model and the experimental data shown in Fig. 6(a) may be a result of energetic disorder in the polymeric material. Previous studies have suggested that the typically large disorder potential ($\sim 100 \text{ meV}$) in conjugated polymer films leads to several deviations from Onsager's theory, including a weaker-than-expected temperature dependence of the photocurrent and an observed onset of the photocurrent at the absorption edge.^{11,20} These effects can result from an energy mismatch between adjacent sites which exceeds the Coulombic binding energy and the thermal energy of the exciton, making its dissociation probability a complex function of the energetic landscape it encounters in the material.

If the value of the lifetime was substantially different from the assumed value of $\tau = 1 \text{ ms}$, then the quantum efficiency from Eq. (2) would be scaled linearly, and different fit parameters would be required. For the $E_\gamma = 2.78 \text{ eV}$ data, a longer lifetime $\tau = 10 \text{ ms}$ results in $r_0 = 1.8 \text{ nm}$ for the Onsager model, while in the Arkhipov model, $l = 3.6 \text{ nm}$ and $\langle E_0 \rangle = 0.025 \text{ eV}$ are necessary.

V. CONCLUSION

In conclusion, we have used terahertz spectroscopy to investigate charge generation in polymer field-effect transistors under illumination. Our measurements show that photoexcited excitons dissociate in the accumulation layer under the application of a gate voltage, with quantum efficiency of ~ 0.1 for an average gate field of $\sim 1 \times 10^8 \text{ V m}^{-1}$. This appears to be the dominant mechanism for generating free charges from excitons, and therefore a photocurrent, in light-sensitive polymer transistors. The quantum efficiency for hole formation from excitons was modeled with the two contrasting models proposed by Onsager and Arkhipov, which are based on dissociation assisted by thermal and electric-

field energy, and an initial excitation of vibrationally excited excitons, respectively. A more comprehensive model of field-induced exciton dissociation in conjugated polymer films will most likely not only have to include effects of the quantum chemical nature of the excited state and its vibrational relaxation dynamics but also the energetic disorder in the material.

ACKNOWLEDGMENTS

The authors would like to acknowledge support from the EPSRC (U.K.) for this work. Surface profilometry measurements were performed with the assistance of C. Baker at BegbrokeNano.

-
- *Present address: ETH Zürich, Institute of Quantum Electronics, Wolfgang-Pauli-Strasse 16 HPT, 8093 Zürich, Switzerland. james.lloyd-hughes@phys.ethz.ch
- †l.herz@physics.ox.ac.uk
- ¹C. J. Brabec, F. Pädinger, N. S. Sariciftci, and J. C. Hummelen, *J. Appl. Phys.* **85**, 6866 (1999).
- ²P. Ravirajan, S. Haque, D. Poplavskyy, J. Durrant, D. Bradley, and J. Nelson, *Thin Solid Films* **451**, 624 (2004).
- ³F. Garnier, R. Hajlaoui, A. Yassar, and P. Srivastava, *Science* **265**, 1684 (1994).
- ⁴H. Sirringhaus, *Adv. Mater. (Weinheim, Ger.)* **17**, 2411 (2005).
- ⁵J. Burroughes, D. Bradley, A. Brown, R. Marks, K. Mackay, R. Friend, P. Burns, and A. Holmes, *Nature (London)* **347**, 539 (1990).
- ⁶S. Barth, H. Bässler, U. Scherf, and K. Müllen, *Chem. Phys. Lett.* **288**, 147 (1998).
- ⁷P. Sreearunothai, A. C. Morteani, I. Avilov, J. Cornil, D. Beljonne, R. H. Friend, R. T. Phillips, C. Silva, and L. M. Herz, *Phys. Rev. Lett.* **96**, 117403 (2006).
- ⁸J. J. M. Halls, A. C. Arias, J. D. MacKenzie, W. Wu, M. Inbasekaran, E. P. Woo, and R. H. Friend, *Adv. Mater. (Weinheim, Ger.)* **12**, 498 (2000).
- ⁹M. Pope and C. E. Swenberg, *Electronic Processes in Organic Crystals and Polymers*, 2nd ed. (Oxford University Press, New York, 1999).
- ¹⁰S. Barth, H. Bässler, H. Rost, and H. H. Hörhold, *Phys. Rev. B* **56**, 3844 (1997).
- ¹¹U. Albrecht and H. Bässler, *Chem. Phys. Lett.* **235**, 389 (1995).
- ¹²G. Dicker, M. P. de Haas, L. D. A. Siebbeles, and J. M. Warman, *Phys. Rev. B* **70**, 045203 (2004).
- ¹³V. I. Arkhipov, E. V. Emelianova, and H. Bässler, *Phys. Rev. Lett.* **82**, 1321 (1999).
- ¹⁴V. I. Arkhipov, E. V. Emelianova, S. Barth, and H. Bässler, *Phys. Rev. B* **61**, 8207 (2000).
- ¹⁵A. Köhler, D. Beljonne, Z. Shuai, J. L. Bredas, A. B. Holmes, A. Kraus, K. Müllen, and R. H. Friend, *Nature (London)* **392**, 903 (1998).
- ¹⁶S. V. Frolov, Z. Bao, M. Wohlgenannt, and Z. V. Vardeny, *Phys. Rev. Lett.* **85**, 2196 (2000).
- ¹⁷R. Kersting, U. Lemmer, M. Deussen, H. J. Bakker, R. F. Mahrt, H. Kurz, V. I. Arkhipov, H. Bässler, and E. O. Göbel, *Phys. Rev. Lett.* **73**, 1440 (1994).
- ¹⁸V. Nikitenko, D. Hertel, and H. Bässler, *Chem. Phys. Lett.* **348**, 89 (2001).
- ¹⁹C. Silva, A. S. Dhoot, D. M. Russell, M. A. Stevens, A. C. Arias, J. D. MacKenzie, N. C. Greenham, R. H. Friend, S. Setayesh, and K. Müllen, *Phys. Rev. B* **64**, 125211 (2001).
- ²⁰S. Barth and H. Bässler, *Phys. Rev. Lett.* **79**, 4445 (1997).
- ²¹K. S. Narayan and N. Kumar, *Appl. Phys. Lett.* **79**, 1891 (2001).
- ²²M. Hamilton and J. Kanicki, *IEEE J. Sel. Top. Quantum Electron.* **10**, 840 (2004).
- ²³A. Salleo and R. Street, *J. Appl. Phys.* **94**, 471 (2003).
- ²⁴L. Bürgi, T. Richards, M. Chiesa, R. Friend, and H. Sirringhaus, *Synth. Met.* **146**, 297 (2004).
- ²⁵L. Bürgi, T. Richards, R. Friend, and H. Sirringhaus, *J. Appl. Phys.* **94**, 6129 (2003).
- ²⁶J. Lloyd-Hughes, T. Richards, H. Sirringhaus, E. Castro-Camus, L. M. Herz, and M. B. Johnston, *Appl. Phys. Lett.* **89**, 112101 (2006).
- ²⁷R. A. Kaindl, M. A. Carnahan, J. Orenstein, D. S. Chemla, H. M. Christen, H. Y. Zhai, M. Paranthaman, and D. H. Lowndes, *Phys. Rev. Lett.* **88**, 027003 (2001).
- ²⁸P. Parkinson, J. Lloyd-Hughes, Q. Gao, H. H. Tan, C. Jagadish, M. B. Johnston, and L. M. Herz, *Nano Lett.* **7**, 2162 (2007).
- ²⁹R. R. Chance and C. L. Braun, *J. Chem. Phys.* **59**, 2269 (1973).
- ³⁰C. Schmuttenmaer, *Chem. Rev. (Washington, D.C.)* **104**, 1759 (2004).
- ³¹J. Lloyd-Hughes, S. K. E. Merchant, F. Lan, H. H. Tan, C. Jagadish, E. Castro-Camus, and M. B. Johnston, *Appl. Phys. Lett.* **89**, 232102 (2006).
- ³²E. Hendry, J. M. Schins, L. P. Candeias, L. D. A. Siebbeles, and M. Bonn, *Phys. Rev. Lett.* **92**, 196601 (2004).
- ³³M. Hamilton, S. Martin, and J. Kanicki, *IEEE Trans. Electron Devices* **51**, 877 (2004).
- ³⁴Y. Y. Noh, D. Y. Kim, and K. Yase, *J. Appl. Phys.* **98**, 074505 (2005).
- ³⁵S. M. Sze, *Physics of Semiconductor Devices*, 2nd ed. (Wiley, New York, 1981).
- ³⁶P. Ravirajan, S. A. Haque, J. R. Durrant, D. Poplavskyy, D. D. C. Bradley, and J. Nelson, *J. Appl. Phys.* **95**, 1473 (2004).
- ³⁷L. Onsager, *Phys. Rev.* **54**, 554 (1938).
- ³⁸D. M. Pai and R. C. Enck, *Phys. Rev. B* **11**, 5163 (1975).
- ³⁹S. F. Alvarado, P. F. Seidler, D. G. Lidzey, and D. D. C. Bradley, *Phys. Rev. Lett.* **81**, 1082 (1998).
- ⁴⁰A. C. Morteani, P. Sreearunothai, L. M. Herz, R. H. Friend, and C. Silva, *Phys. Rev. Lett.* **92**, 247402 (2004).